View metadata, citation and similar papers at core.ac.uk

brought to you by CORE

provided by Elsevier - Publisher Connector

Solution structure of the sodium channel antagonist conotoxin GS: a new molecular caliper for probing sodium channel geometry

Justine M Hill, Paul F Alewood and David J Craik*

Background: The venoms of *Conus* snails contain small, disulfide-rich inhibitors of voltage-dependent sodium channels. Conotoxin GS is a 34-residue polypeptide isolated from *Conus geographus* that interacts with the extracellular entrance of skeletal muscle sodium channels to prevent sodium ion conduction. Although conotoxin GS binds competitively with μ conotoxin GIIIA to the sodium channel surface, the two toxin types have little sequence identity with one another, and conotoxin GS has a four-loop structural framework rather than the characteristic three-loop μ-conotoxin framework. The structural study of conotoxin GS will form the basis for establishing a structure–activity relationship and understanding its interaction with the pore region of sodium channels.

Results: The three-dimensional structure of conotoxin GS was determined using two-dimensional NMR spectroscopy. The protein exhibits a compact fold incorporating a β hairpin and several turns. An unusual feature of conotoxin GS is the exceptionally high proportion (100%) of *cis*-imide bond geometry for the three proline or hydroxyproline residues. The structure of conotoxin GS bears little resemblance to the three-loop μ conotoxins, consistent with the low sequence identity between the two toxin types and their different structural framework. However, the tertiary structure and cystine-knot motif formed by the three disulfide bonds is similar to that present in several other polypeptide ion channel inhibitors.

Conclusions: This is the first three-dimensional structure of a 'four-loop' sodium channel inhibitor, and it represents a valuable new structural probe for the pore region of voltage-dependent sodium channels. The distribution of amino acid sidechains in the structure creates several polar and charged patches, and comparison with the μ conotoxins provides a basis for determining the binding surface of the conotoxin GS polypeptide.

Address: Centre for Drug Design and Development, The University of Queensland, Brisbane, Queensland 4072, Australia.

*Corresponding author.
E-mail: d.craik@mailbox.uq.oz.au

Key words: *cis*-peptide bond, γ-carboxyglutamic acid, γ-*trans*-hydroxyproline, NMR spectroscopy, μ conotoxin

Received: 31 January 1997
Revisions requested: 25 February 1997
Revisions received: 10 March 1997
Accepted: 10 March 1997

Electronic identifier: 0969-2126-005-00571

Structure 15 April 1997, 5:571–583

© Current Biology Ltd ISSN 0969-2126

Introduction

Excitable tissues such as nerve, skeletal muscle and heart contain voltage-dependent sodium channels that play an important role in the generation of the action potentials responsible for electrical signalling. Several groups of neurotoxins that bind with high affinity and high specificity to these channels have been used as probes for both structural and functional studies [1,2]. These toxins exert several effects that range from blocking the open channel to extensive modification of the channel's gating and permeation properties. Of particular interest are channel blockers, including the small guanidinium toxins, tetrodotoxin (TTX) and saxitoxin (STX), and several polypeptide toxins isolated from the venoms of *Conus* snails. Most channel blockers bind with 1:1 stoichiometry to the extracellular entrance of the channel (site I) to occlude the pore and prevent sodium ion conduction [1,2]. TTX, STX and μ conotoxin GIIIA have been valuable as probes to map residues in the pore region of sodium channels [3–8].

The piscivorous cone snail *Conus geographus* produces polypeptide neurotoxins that specifically inhibit skeletal muscle and eel electroplax sodium channels [9–11]. These toxins, the μ conotoxins and conotoxin GS, are particularly useful probes of sodium channel structures because of their high binding affinity and their ability to discriminate between the skeletal muscle, neuronal and cardiac channel isoforms [9–14]. Significantly, although these peptides belong to the same pharmacological class, they have different structural frameworks, as illustrated in Figure 1. The μ conotoxins, a family of highly basic 22-residue polypeptides (GIIIA, GIIIB and GIIIC), contain six cysteine residues that are paired in a 1–4, 2–5, 3–6 pattern to form three intramolecular disulfide bonds and a three-loop framework. Conotoxin GS has a strikingly different sequence and is 50% larger than the μ conotoxins; it contains six cysteine residues arranged in a similar 1–4, 2–5, 3–6 pattern [15], but differences in the spacings between cysteine residues results in a four-loop framework rather than a three-loop framework (Fig. 1). Despite the

Figure 1

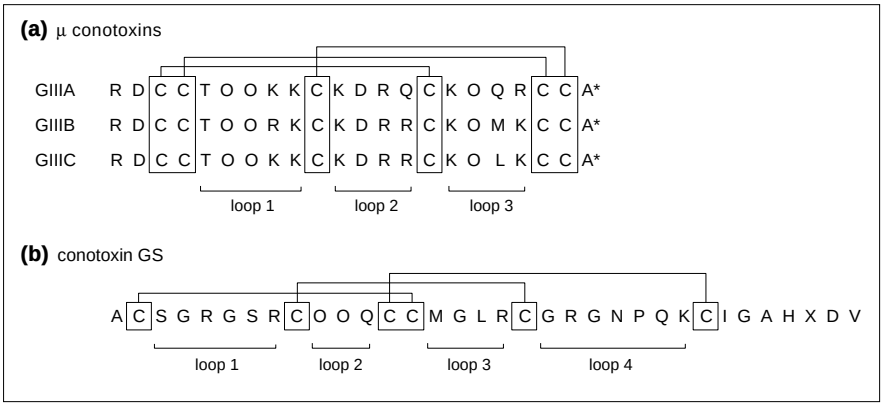

Primary sequences of the sodium-channel blocking conotoxins from *Conus geographus*. O is γ-*trans*-L-hydroxyproline; X is γ-carboxy-L-glutamic acid; * is an amidated C terminus. These polypeptides contain either **(a)** a three-loop framework as in the μ conotoxins or **(b)** a four-loop framework as in conotoxin GS. The cysteine residues are boxed to emphasize their role in defining the framework, and the loops indicated comprise the polypeptide backbone between cysteine residues.

low sequence identity between conotoxin GS and μ conotoxin GIIIA, the two toxins bind competitively, suggesting overlapping binding sites on the extracellular surface of skeletal muscle and eel electroplax sodium channels [11].

The three-dimensional solution structures of μ conotoxins GIIIA [16–18] and GIIIB [19] have been determined, revealing a common backbone fold consisting of a small β hairpin, a distorted 3_{10} helix and several turns. However, there is no information available on the three-dimensional structures of sodium-channel blockers with a four-loop framework, such as conotoxin GS. Determination of the structure of conotoxin GS is therefore important, in order to obtain further insights into the interactions of these toxins with the pore region of sodium channels.

Conotoxin GS is composed of 34 residues, including two post-translationally modified amino acids — γ-*trans*-hydroxyproline (Hyp) at positions 10 and 11 and γ-carboxyglutamic acid (Gla) at position 32. Although the presence of post-translational modifications — in particular hydroxyproline — is a common feature of conotoxins, a definitive explanation of their role remains unknown. Gla has also been found in other *Conus* peptides, most notably in the conantokins which have *N*-methyl-D-aspartate (NMDA) receptor antagonist activity [20]. The conantokins differ from other *Conus* peptides in that they lack disulfide bonds, but instead they contain four or five γ-carboxyglutamic acid residues, leading to the suggestion that these residues are responsible for stabilizing their α-helical conformation in the presence of calcium ions [21,22]. There are now examples of peptides containing both disulfide bonds and multiple γ-carboxyglutamic acid residues, however, ([23] and J-P Bingham, personal communications), and it is becoming more important to determine the structural or functional significance of this post-translational modification.

In this paper, we describe the three-dimensional structure of conotoxin GS in aqueous solution, determined using 2D ^{1}H NMR spectroscopy. The structure provides the basis for mapping the channel-binding surfaces of this polypeptide which will in turn allow the pore region of voltage-dependent sodium channels to be probed. To gain an insight into the role of γ-carboxyglutamic acid, in this peptide, we have studied the effect of calcium ions on the structure and investigated the solution structure of an analog ([Glu32]conotoxin GS) in which Gla32 was replaced with glutamic acid.

Results

Conotoxin GS and [Glu32]conotoxin GS were prepared by solid-phase peptide synthesis, and the disulfide bonds were introduced by air oxidation in the presence of reduced and oxidised glutathione, as described by Nakao *et al.* [15]. Analytical reverse-phase HPLC and electrospray ionization mass spectrometry confirmed the purity and molecular weight of the synthetic peptides.

Resonance assignment

The sequence-specific resonance assignment of conotoxin GS was achieved according to the method described by Wüthrich [24], using a combination of DQF-COSY, TOCSY and NOESY spectra at 25°C. Any ambiguities due to overlap were resolved from analogous spectra recorded at 15°C. The large chemical shift dispersion of backbone ^{1}H resonances provides the first indication of a well-defined structure in solution. This is illustrated in the DQF-COSY and NOESY spectra shown in Figure 2. In the fingerprint region of the DQF-COSY spectrum, cross peaks corresponding to intraresidue NH–Hα connectivities are observed for all backbone amide protons, except for Cys19 and His31 which are overlapped with the water resonance. Sequential connectivities observed in the NOESY spectrum were used to align the identified spin systems according to the primary sequence of the molecule. The Hα–NH_{i+1} connectivities for residues 1–9, 11–23 and 24–34 are illustrated in the NOESY spectrum in Figure 2b.

Figure 2

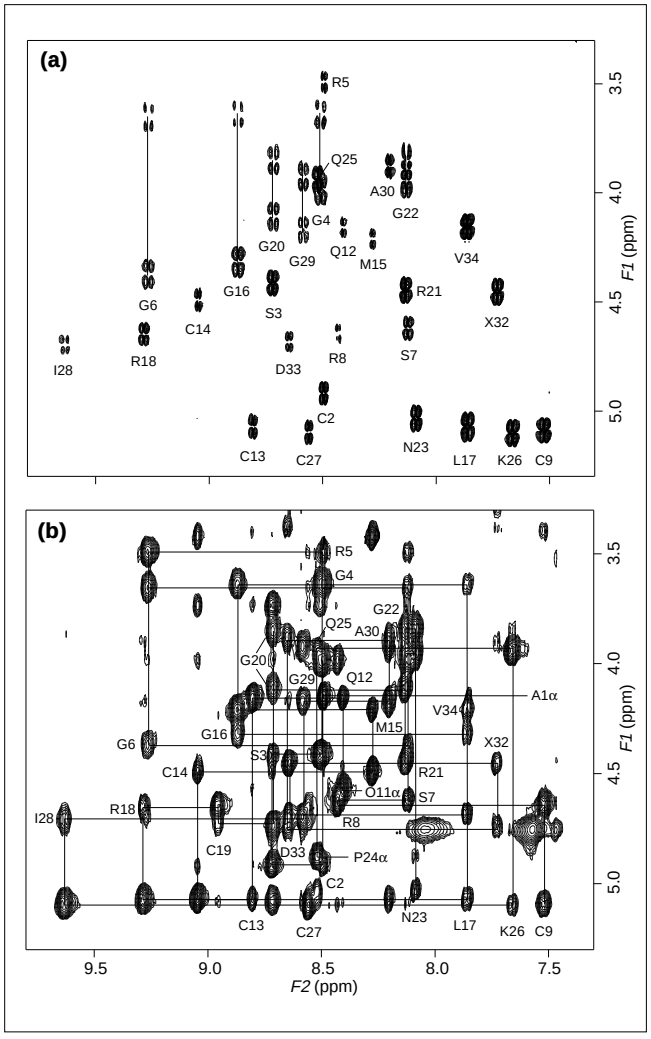

Fingerprint regions of (a) DQF-COSY and (b) 250 ms NOESY spectra of 2 mM conotoxin GS in 90% H_2O/10% D_2O at 25°C, pH 2.9. In the DQF-COSY spectrum (a), cross peaks correspond to intraresidue NH–Hα connectivities; solid lines indicate pairs of peaks for glycine residues. In the NOESY spectrum (b), Hα–NH_{i+1} connectivities (solid lines) are shown for residues 1–9, 11–23, and 24–34; intraresidue NH–Hα cross peaks are marked with the one-letter code for the amino acid and the residue number.

Conotoxin GS contains two hydroxyproline residues and one proline residue which interrupt the sequential Hα–NH_{i+1} connectivities. The Cys9–Hyp10 and Asn23–Pro24 peptide-bond conformations are both *cis*, as inferred from the presence of strong Hα–$Hα_{i+1}$ cross peaks in the NOESY spectrum recorded in D_2O [24]. The chemical shift degeneracy of the Hα protons of Hyp10 and Hyp11 prevented the observation of either Hα–$Hδ_{i+1}$ or Hα–$Hα_{i+1}$ connectivities for Hyp11, making it impossible to determine the conformation of the Hyp10–Hyp11 peptide bond unambiguously from ^{1}H-NMR data. However, ^{13}C-NMR data for Hyp11 suggested a *cis*-peptide bond based on the chemical shift dispersion of the Cβ and Cγ resonances [19,25,26]. Hyp11 has a chemical shift dispersion value ($Δδ_{Cγ–Cβ}$) of 30.8 ppm, as determined from the HMQC spectrum; this is consistent with the *cis* but not the *trans* form, for which a chemical shift dispersion of ~33 ppm would be expected [19]. The ^{13}C chemical shifts also confirmed the *cis*-peptide bonds for Hyp10 ($Δδ_{Cγ–Cβ}$ = 28.1 ppm) and Pro24 ($Δδ_{Cγ–Cβ}$ = 9.6 ppm), thus providing a useful adjunct to ^{1}H-NMR data in determining the peptide-bond conformation for these residues. It is interesting, and unprecedented in comparisons with similar-sized polypeptides, that all three of the proline/hydroxyproline residues of conotoxin GS are in the *cis* conformation.

Stereospecific assignments for the β-methylene protons and $χ_1$-angle restraints (given in parentheses) were determined for eight residues — Cys2, Cys9 (+60±30°); Cys13, Cys14, Leu17, Cys27 (–60±30°); and Cys19, Gla32 (180±30°) by analysis of $^3J_{Hα–Hβ}$ values and NOE intensity patterns [27]. A complete list of the ^{1}H- and ^{13}C-resonance assignments is available as supplementary material (published with the internet version of this paper).

Secondary structure

A qualitative analysis of the sequential and medium range NOEs, $^3J_{NH–Hα}$ coupling constants, amide-NH exchange rates, and secondary Hα chemical shifts was used to characterize the secondary structure of conotoxin GS. These data, summarized in Figure 3, indicate that the major secondary structure feature is antiparallel β strands, comprising residues 7–9, 17–20 and 26–29. Several parameters are consistent with this determination — strong sequential Hα–NH_{i+1} connectivities, weak NH–NH_{i+1} connectivities and a number of interstrand NOEs; medium or slow amide exchange rates; $^3J_{NH–Hα}$ coupling constants greater than 8 Hz; and Hα chemical shift indices of +1 [28]. Four Hα–NH, three Hα–Hα and five NH–NH connectivities were observed between strands, allowing the tentative identification of six hydrogen bonds as illustrated in Figure 3. The $^3J_{NH–Hα}$ coupling constants for Arg8 and Cys27, however, are smaller than expected for canonical ϕ angles found in β sheets, suggesting deviations from idealized structure for these residues. The presence of several medium range Hα–NH_{i+2} and NH–NH_{i+2} NOEs for the remainder of the sequence suggests that the structure also consists of several turns. These are described in detail below.

The disulfide connectivities of the synthetic peptide were confirmed by an examination of the NOEs between cysteine residues [29]. Disulfide bridges between residues Cys2–Cys14, Cys9–Cys19 and Cys13–Cys27 were indicated by the following NOEs: Cys2Hβ–Cys14Hα (strong intensity), Cys9Hβ–Cys19Hβ (medium intensity) and Cys13Hβ–Cys27Hβ (medium intensity). This pattern of disulfide bridges is consistent with that determined chemically [15],

Figure 3

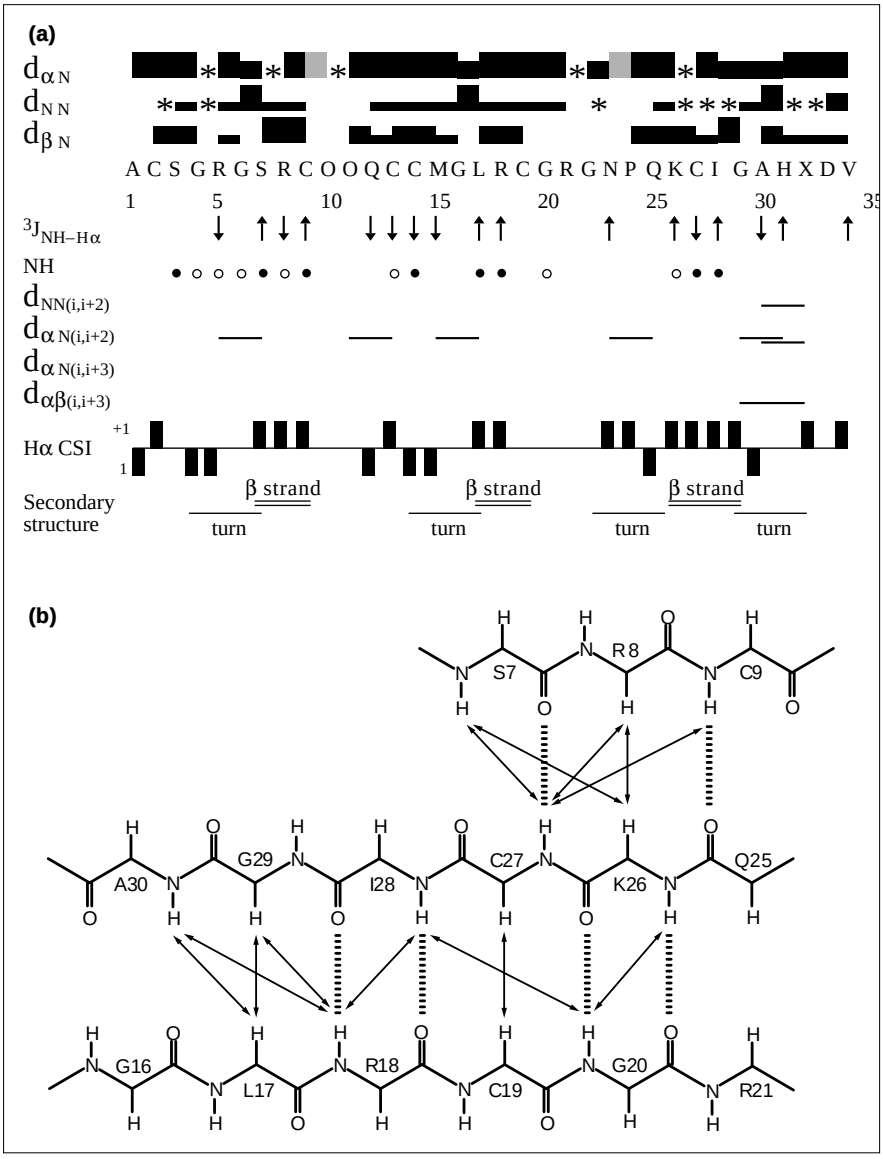

Summary of the NMR data used for characterizing the secondary structure of conotoxin GS. (a) Solid bars indicate sequential connectivities observed in a 250 ms NOESY spectrum at 25°C, pH 2.9. Shaded bars correspond to $H\alpha–H\alpha_{i+1}$ connectivities for hydroxyproline and proline residues. The height of the bar indicates the strength of the NOE. Overlapping NOEs are indicated by an asterisk (*); ↓ indicate $^3J_{NH-H\alpha}$ coupling constants ≤5 Hz; ↑ indicate $^3J_{NH-H\alpha}$ coupling constants ≥8 Hz. Open circles indicate backbone NH protons that did not exchange with D_2O after 4 h; filled circles indicate NH protons that did not exchange after 24 h. A chemical shift index (CSI) of –1 or +1 for Hα protons indicates a shift deviation from the random-coil value of greater than 0.1 ppm upfield or downfield, respectively, and those within the range of the random coil are indicated by a CSI of 0 [28]. A grouping of four or more successive +1 indices is often taken as evidence of β sheet. (b) Schematic diagram of the β strands in conotoxin GS showing the interstrand NOEs (arrows), and inferred hydrogen bonds (broken lines). Note that the C9NH–Q25CO hydrogen bond is tentatively proposed based on the slow exchange and NOE data, but is not supported by the three-dimensional structure calculations (see text).

and is common to other conotoxins with the six-cysteine and four-loop framework [20,30].

Structure determination

A set of 50 three-dimensional structures was calculated using 487 interproton distance restraints derived from 211 intraresidual, 114 sequential, 43 medium range (|i-j|≤5) and 119 long range NOEs. These restraints were supplemented with 17 backbone and 8 sidechain dihedral angle restraints from spin–spin coupling constants and 18 distance restraints defining 9 hydrogen bonds. The 20 structures with the lowest energies were chosen to represent the solution structure of conotoxin GS (Fig. 4). The geometric and energetic statistics of the final structures, given in Table 1, show that the structures satisfy the experimental restraints and exhibit only small deviations from idealized geometry.

Residues 2–20 and 25–31 of the final structures were found to have well defined backbone dihedral angles (S>0.9) and low root mean square (rms) deviations for the backbone atoms (Fig. 5). The residues with higher atomic rms deviations and lower angular order parameters correspond to the N and C termini and the loop region between the strands in the β hairpin. This is reflected in the small number of medium range NOEs and absence of long range NOEs for these regions of the molecule (Fig. 5). The mean pairwise rms deviations for the backbone heavy atoms (N, Cα and C) and all heavy atoms were 1.10±0.31 and 2.09±0.35 Å, respectively, whereas

Figure 4

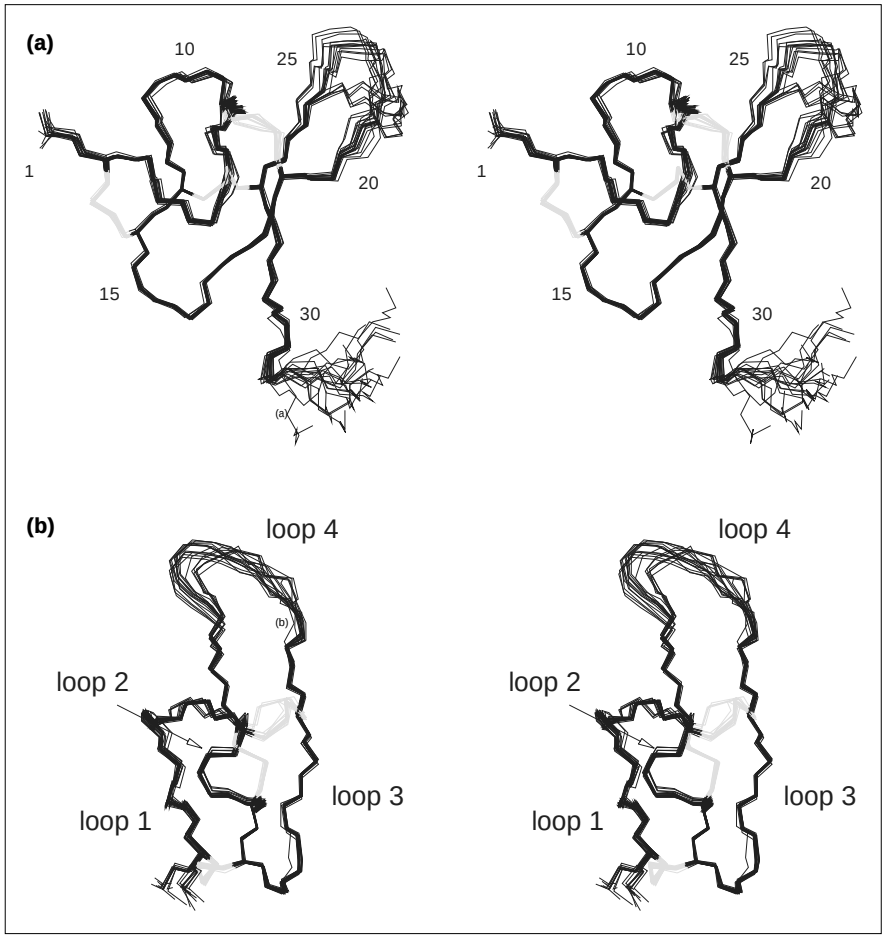

The three-dimensional structure of conotoxin GS. (a) Stereo view of the 20 final structures superimposed over the backbone (C, Cα and N) atoms of the well-defined region encompassing residues 2–20 and 25–31. The three disulfide bonds (2–14, 9–19 and 13–27) are shown in lighter grey. (b) Stereoview illustrating the orientation of the four loops in the structure. For clarity, the C-terminal residues 28–34 are not shown. This figure was produced using Insight II (version 95.0.3, Biosym Technologies).

the corresponding values for residues 2–20 and 25–31 were 0.34±0.13 and 1.27±0.19 Å. In addition, all residues with a well defined backbone conformation are located within the allowed regions of the Ramachandran plot.

Description of the structure

The three-dimensional structure of conotoxin GS consists of a compact disulfide-bonded core, from which several loops and the C terminus project (Fig. 4). The main element of regular secondary structure is a double-stranded antiparallel β sheet comprising residues 17–20 and 26–29, which are connected by a turn (residues 21–25) that forms a β-hairpin structure. A further peripheral β strand composed of residues 7–9 is almost perpendicular to the β hairpin, with only Ser7 hydrogen bonded to the central β strand forming an isolated β bridge [31]. Although the NOEs (Fig. 3) are consistent with these residues forming a third β strand, it does not constitute a complete β sheet as only Ser7 and Cys9 have ϕ,ψ angles that are characteristic of a β strand, and the expected hydrogen bond between Cys9NH and Gln25CO is not present in any of the calculated structures. An interesting feature of the structure is an additional β bridge between residues Ser3 and Cys13, which is formed by hydrogen bonds Ser3NH–Gln12CO and Cys14NH–Ser3CO, and which provides further stability to the N terminus of the molecule.

The elements of β structure are linked by turns involving residues 4–7, 9–12, 14–17, 22–25 and 29–32. The β turns were identified on the criterion that the distance between the Cα atoms of residues *i* and *i*+3 is less than 7 Å and the central residues are not helical [32]. At the N terminus, residues 4–7 (loop 1) form a type II β turn (ϕ_2, $\psi_2 = -65°$, 98° and ϕ_3, $\psi_3 = 143°$, –12°). Between the β bridge at Ser7 and the β hairpin are two turns, involving residues 9–12 (loop 2) and 14–17 (loop 3). The first turn, involving residues 9–12, is non-standard and has two *cis* hydroxyprolines as the central residues. The average ϕ, ψ angles for Hyp10 and Hyp11 are –75°, 174° and –58°, 134°, respectively, such that the turn is classified as $\beta_p\beta_p$ [33]. A second turn involving residues 14–17 may be classified as type II (ϕ_2, $\psi_2 = -55°$, 128° and ϕ_3, $\psi_3 = 104°$, –29°). The strands in the β hairpin are connected by a relatively disordered loop from Arg21 to Gln25 (loop 4). The average ϕ, ψ

Table 1

Geometric and energetic statistics for the 20 solution structures of conotoxin GS*.

Rms deviations from experimental restraints†	
interproton distances (Å) (487)	0.048 ± 0.003
dihedral angles (°) (25)	0.167 ± 0.073
Rms deviations from idealised geometry	
bonds (Å)	0.007 ± 0.001
angles (°)	2.20 ± 0.04
impropers (°)	0.17 ± 0.01
Energies (kcal mol^{-1})‡	
E_{total}	–81.9 ± 5.8
E_{NOE}	11.4 ± 1.4
E_{cdih}	0.05 ± 0.03
E_{L-J}	–135.2 ± 3.2
$E_{bond} + E_{angle} + E_{improper}$	64.2 ± 2.4
Pairwise rms deviations for backbone atoms (N, Cα and C) (Å)	
1–34	1.10 ± 0.31
2–20, 25–31	0.34 ± 0.13

*The values in the table are the mean ± standard deviation. †The number of restraints is shown in parentheses. None of the structures had distance violations > 0.3 Å or dihedral angle violations > 3°. ‡Force constants for the calculation of square-well potentials for the NOE and dihedral angle restraints were 50 kcal mol^{-1} Å^{-2} and 200 kcal mol^{-1} rad^{-2}, respectively. The Lennard–Jones van der Waals energy was calculated with the CHARMM empirical energy function [55].

Figure 5

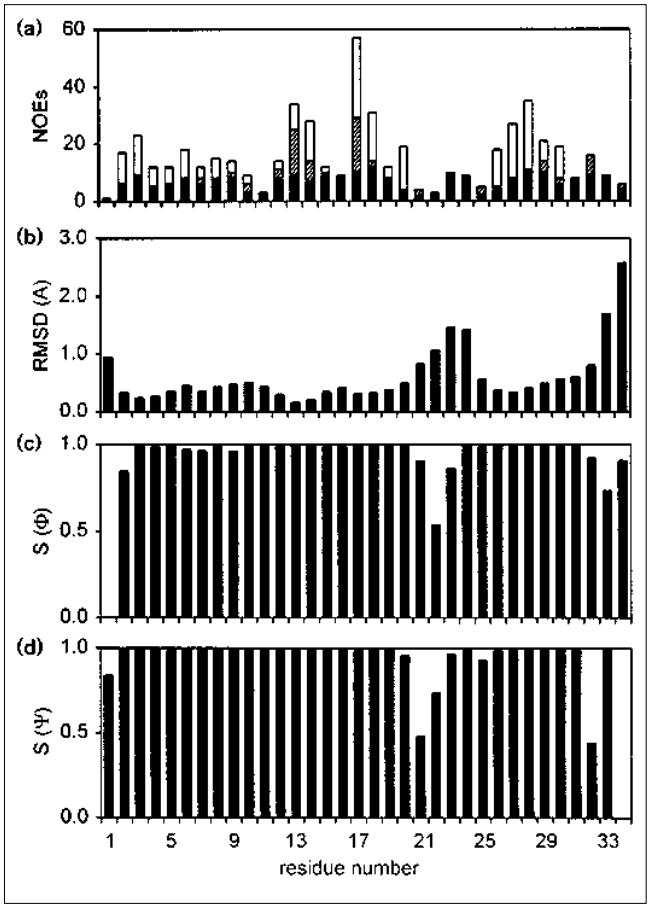

Parameters characterizing the 20 final structures of conotoxin GS, plotted as a function of residue number. (a) NOE restraints. Sequential, medium-range ($|i-j| \pm 5$) and long-range NOEs are indicated by filled, cross-hatched and open bars, respectively. (b) Rms deviations from the average structure for the backbone atoms. (c,d) Angular order parameters [44] for the backbone dihedral angles ϕ and Ψ.

angles for Asn23 and Pro24 are –143°, 110° and –72°, 132°, respectively, indicating that on average the correct geometry for a type VIb turn exists. Examination of the individual structures within the calculated ensemble, however, shows that this region is represented by two conformations — either a type VIb turn (14 structures) or a nonstandard $\beta_p\beta_p$ turn (six structures). Conformational mobility between the two turn types may be responsible for the disorder in this region of the molecule, but the relatively small number of NOEs in this region makes it difficult to determine whether a true two-state equilibrium exists. Finally, residues 29–32 following the β hairpin adopt a type I β turn (ϕ_2, $\psi_2 = -80°$, –43° and ϕ_3, $\psi_3 = -94°$, 44°).

Hydrogen bonds associated with these secondary structure elements account for many of the observed slowly exchanging backbone amide protons. The network of hydrogen bonds between β strands, identified by qualitative analysis of the data (Fig. 3), is present in the calculated structures, with the exception of Cys9NH which lacks a clearly defined hydrogen-bonding partner. However, Cys9 is substantially buried from the solvent, which accounts for the slowed exchange of its amide proton. The type II turns are stabilized by hydrogen bonds between the carbonyl group (*i*) and the amide proton (*i*+3) of the peptide backbone, whereas the expected hydrogen bond in the type I turn at the C terminus is formed in only 50% of the structures. This is consistent with the fast exchange rate observed for the amide proton of Gla32, which is probably due to higher solvent exposure and conformational flexibility of this region relative to the core of the molecule.

The structure of conotoxin GS is stabilized by three disulfide bonds (2–14, 9–19 and 13–27). The conformation of the 2–14 and 13–27 disulfide bonds is well defined (Fig. 4), and their torsion angles are representative of a right-handed hook and left-handed spiral, respectively [31]. The 9–19 disulfide bond is less well defined and appears to be represented by two conformations, with sixteen structures displaying a left-handed conformation and four structures having a right-handed spiral conformation. The three disulfide bonds form a knot in which the 13–27 disulfide bond passes through a ring formed by the other two disulfides and the connecting polypeptide backbone [34]. Disulfides 9–19 and 13–27 are shielded from the solvent and contribute to a small hydrophobic core which also includes Leu17, Gly20, Ile28 and Gly29.

Role of the γ-carboxyglutamic acid residue

To investigate the role of Gla32 in this polypeptide, an analog — [Glu32]conotoxin GS — was synthesized and the NMR spectra compared with those of conotoxin GS. The chemical shift differences for the backbone Hα and NH protons of conotoxin GS and [Glu32]conotoxin GS were small (≤0.05 ppm), suggesting that the backbone conformation of the two peptides is essentially identical. Several other parameters, including the observed NOEs, $^3J_{NH-H\alpha}$ coupling constants and amide exchange rates are similar, providing further evidence of conserved structure in the two peptides.

We have also studied the effects of trifluoroethanol and calcium ions on the structure of conotoxin GS. The C terminus of conotoxin GS has been predicted to form α helix [11], but in the hydrophobic environment provided by trifluoroethanol no conformational change in this region of the molecule was observed. The effects of calcium ions on the Hα shifts were also minimal, indicating that there was no significant conformational change in the presence of calcium. In addition, calcium did not affect the sidechain resonances of Gla32 and there was no evidence of line broadening to suggest an interaction with calcium. This result may be explained by the fact that the single γ-carboxyglutamic acid residue in conotoxin GS is outside the cysteine-rich portion, and consequently it may not play a crucial role in either the structure or the function of this polypeptide. By contrast, the function of other γ-carboxyglutamic acid-containing peptides and proteins, especially those containing Gla–Gla pairs, is dependent on the binding of calcium ions [21].

Discussion

The three-dimensional structure of conotoxin GS consists of a β hairpin, involving residues 17–29, and several turns. The structure is stabilized by three disulfide bonds and a number of intramolecular hydrogen bonds. Several of the secondary structure elements have nonstandard geometries, typical of small disulfide-rich proteins.

An interesting feature of conotoxin GS is the presence of the two post-translationally modified amino acids, γ-*trans*-hydroxyproline and γ-carboxyglutamic acid. The two hydroxyproline residues and one proline residue were determined to be in the *cis*-peptide bond conformation. This unusual and exceptionally high proportion (100%) of *cis* imide geometry for the proline/hydroxyproline residues suggests a structural significance for this geometry in conotoxin GS. Although there has been no systematic analysis of the geometry of hydroxyproline, it has been found that ~6% of X–Pro imide bonds in the Brookhaven Protein Data Bank (PDB) are in the *cis* conformation [35,36]. *Cis*-imide bonds are found primarily in bends and turns, suggesting a specific structural role for this type of bond [35,36]. In conotoxin GS, Hyp10 and Hyp11 comprise the central residues of a non-standard turn, while Pro24 is in the *i*+2 position of a type VIb turn. The driving force for *cis* geometry in the two turns appears to be different. Loop 2, containing Hyp10 and Hyp11, forms a turn immediately followed by a disulfide-bonded cysteine residue, and the geometry is tightly constrained to place Cys13 in the correct orientation to form a disulfide bond with Cys27 (Fig. 4). Loop 2 simply appears to be too short to accommodate the more common *trans*-imide geometry, despite the fact that *cis* geometry following a cysteine residue appears to be generally unfavourable as judged by its low incidence (2.5%) in the PDB [35]. The presence of Pro24 in a type VIb turn (loop 4) is consistent with previous observations that a high proportion of X–*cis* Pro occurrences in globular proteins are found as type VI turns [32].

γ-Carboxyglutamic acid residues in peptides and proteins have been implicated in binding both calcium ions and membranes. The γ-carboxyglutamic acid residue at position 32 in conotoxin GS, however, does not appear to play a crucial structural role as the addition of calcium ions does not induce a conformational change, and the residue may be substituted by a glutamic acid without significantly altering the structure. These results support the study by Nakao *et al.* [15], who reported similar circular dichroism spectra for [Glu32]conotoxin GS and conotoxin GS, both in the presence and absence of calcium ions. Nakao *et al.* [15] also suggested that Gla32 may not be important for activity, as conotoxin GS and [Glu32]conotoxin GS have essentially the same toxicity in fish. In the calculated structures, the sidechain of Gla32 is in close proximity to the sidechain of Arg5. The proximal arrangement of these sidechains is strongly supported by the high-field chemical shift of the Hα proton of Arg5 (0.9 ppm upfield from its random coil value). Further support for a fixed conformation of these residues is that the Hδ protons of Arg5 are non-degenerate. A likely reason for the position of Gla32 is its participation in a hydrogen bond with Arg5, although this may also occur when glutamic acid is at this position.

Comparison with the 'three-loop' μ conotoxins

The structure of conotoxin GS bears little resemblance to the three-loop μ conotoxins GIIIA [16–18] and GIIIB [19], consistent with the low sequence identity between conotoxin GS and the μ conotoxins and their different cysteine frameworks. Figure 6 shows the secondary structure found in the two types of sodium channel blocking conotoxins from *C. geographus*. The main structural feature in the three-loop μ conotoxins is a distorted 3_{10} helix comprising residues 13–22, whereas conotoxin GS consists predominantly of β strands and turns. Despite these significant structural differences, conotoxin GS binds competitively with μ conotoxin GIIIA, suggesting that they have overlapping binding sites on the sodium channel surface [11]. Thus, a similar spatial distribution of functionally important sidechains may have evolved on these different structural scaffolds.

Figure 6

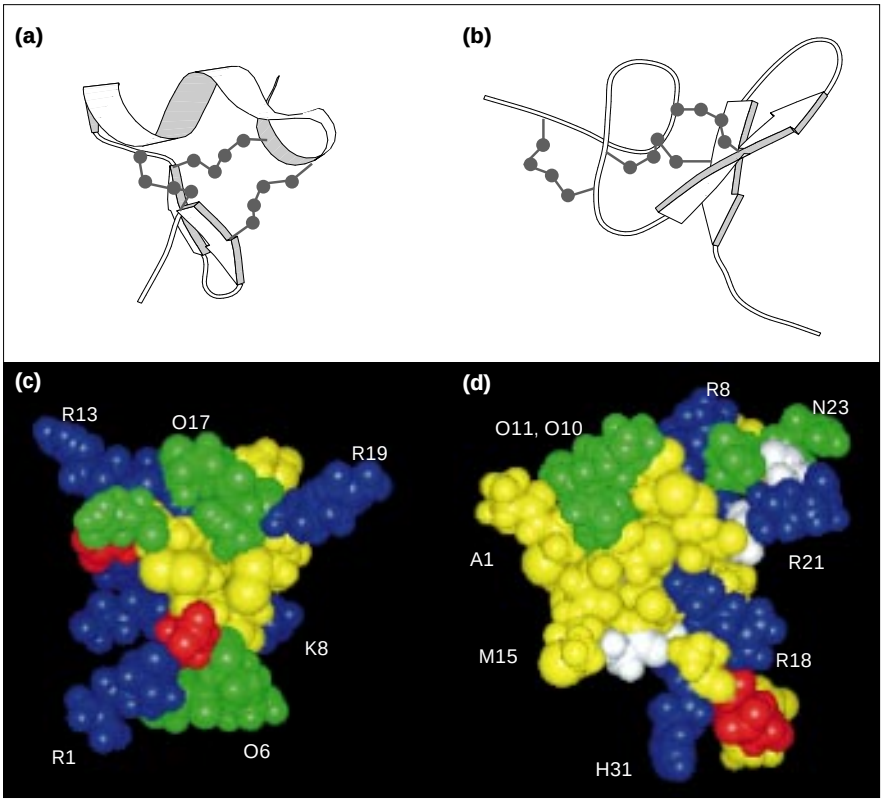

Comparison of the structure of the sodium-channel blocking conotoxins from *Conus geographus*. The upper panel shows schematic representations of the structure of (a) μ conotoxin GIIIA [18]; PDB accession code 1TCG) and (b) conotoxin GS, highlighting the elements of secondary structure and disulfide bonds; β strands are shown as wide arrows and the 3_{10} helix as a coil, with disulfide bonds represented by ball-and-stick models. The lower panel shows space-filling models of (c) μ conotoxin GIIIA and (d) conotoxin GS. Residues are coloured as follows: positively charged (blue), negatively charged (red), uncharged hydrophilic (green), hydrophobic (yellow), and glycine (white). The figure was produced using the programs MOLSCRIPT [58] and Insight II (version 95.0.3, Biosym Technologies).

Voltage-dependent sodium channels are comprised of four homologous domains, each containing six putative α-helical transmembrane segments, S1 to S6, and a membrane-associated loop between S5 and S6. Each of the four domains contributes a loop to the ion conduction pore, which is bounded at its external and internal entrances by wide vestibules. The pore loops contain residues involved in ion selectivity and conduction, and they also form the binding site for many sodium-channel blockers [3–7,14]. Extensive mutagenesis of μ conotoxin GIIIA revealed that the basic nature of the molecule is a crucial factor for activity, with substitutions of Arg13 having the largest effect on binding affinity [8,37,38]. These results demonstrate that a guanidinium group is necessary for blockade of the channel, as is also the case for TTX and STX. Several residues (Lys16, Hyp17 and Arg19) in loop 3 of GIIIA also appear to be important for activity. These residues, like Arg13, are located in the 3_{10} helix, and this face of the molecule has been suggested to interact with the sodium channel [18]. Recent studies using a complementary mutagenesis strategy have begun to reveal pairs of interacting toxin–channel residues [7,8]. Dudley *et al.* [7] have proposed a model for the interaction of μ conotoxin GIIIA with the outer vestibule of the sodium channel based on the available binding data. Their model predicts that μ conotoxin GIIIA occludes the pore by the guanidinium group of Arg13 interacting with two carboxyl groups at the putative selectivity filter (Asp400 and Glu755), with the association rate of the toxin increased by interaction with Glu758. Additional mutations are required to further define the molecular interactions of μ conotoxin GIIIA with the sodium channel.

Conotoxin GS may also be expected to establish electrostatic interactions with the sodium channel, by analogy with μ conotoxin GIIIA, TTX and STX. It is therefore of interest to highlight the location and nature of the charged residues in this polypeptide. Conotoxin GS contains six basic residues (Arg5, Arg8, Arg18, Arg21, Lys26 and His31) and two acidic residues (Gla32 and Asp33) that are localized at the C terminus. All of the positively charged groups are on the surface of the molecule, with His31, Arg21 and Arg5 being the most solvent exposed. The distributions of charged, hydrophobic and polar residues in conotoxin GS and μ conotoxin GIIIA are dissimilar (Fig. 6). In conotoxin GS, an asymmetric distribution of residues forms a charged hydrophilic face, and a small hydrophobic face containing Ala1, Met15 and part of the 2–14 disulfide bond (Figs 6 and 7). The large number of polar residues in conotoxin GS (Ser3, Ser7, Hyp10, Hyp11, Gln12, Asn23 and Gln25) are clustered inone region of the molecule and may play a role in receptor

Figure 7

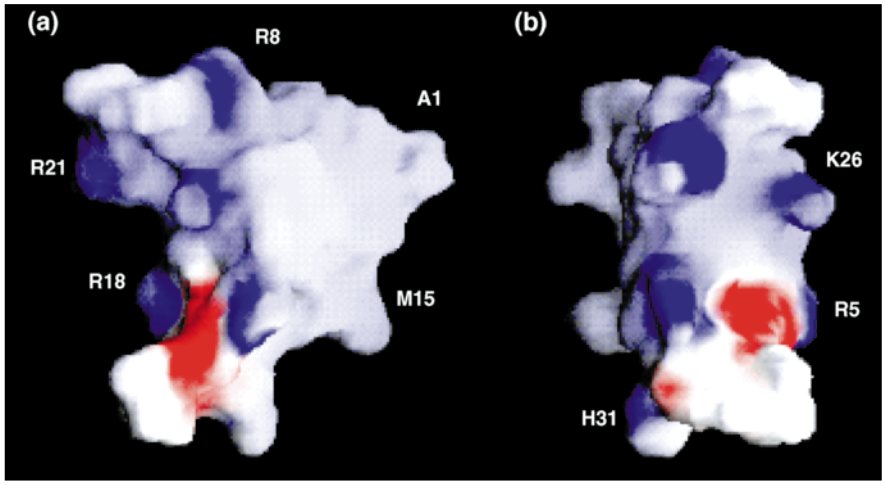

Surface representation of conotoxin GS. Two views of the molecular surface of conotoxin GS, coloured according to electrostatic potential from electronegative to electropositive by a red-to-blue continuous colour range. The view in (a) is related to that in Figure 6d by a rotation of 180° about the vertical axis. The view in (b) is related to that in (a) by a rotation of 90° about the vertical axis. The figure was produced using GRASP [57].

binding by establishing hydrogen-bonding contacts with the sodium channel. A further structural difference between the μ conotoxins and conotoxin GS is the presence of a C-terminal tail in the latter. The additional seven residues in conotoxin GS are an unusual feature, as conotoxins typically contain few, if any, residues outside the cysteine core [20,30]. The C terminus of conotoxin GS is well defined, with residues 28–29 participating in the second strand of the β hairpin and residues 29–32 forming a type I β turn. By contrast, ω agatoxins IVA and IVB, which block P-type calcium channels, have a C-terminal tail that is disordered in solution [39,40]. The importance of the tail to the activity of conotoxin GS is unknown, but it may be significant by analogy with ω agatoxin IVA. In this case, the truncated analog, ω agatoxin IVA(1–40), is 100-fold less potent than the entire molecule in blocking the P-type calcium channel [40].

The variety of sodium-channel blockers is a reflection of the diversity of groups that can fit the antagonist-binding site (or macrosite) of sodium channels. Like μ conotoxin GIIIA and TTX [5], conotoxin GS and GIIIA may not share all of their attachment points on the sodium channel. At present, we can only speculate about the interaction of conotoxin GS with the sodium channel and about which of the basic residues may be directly involved in occluding the sodium conduction pathway. The structural studies reported here provide a valuable background for future mutagenesis studies. On the basis of the conotoxin GS structure, residues that should be investigated include Arg8 and Arg21, which are highly solvent-exposed and located near the polar residues that may also be involved in binding. It would also be of interest to examine a truncated molecule to assess the role of the C-terminal tail and the anionic cluster in this region.

Comparison with other polypeptide toxins

Conotoxins with the six-cysteine and four-loop framework, as in conotoxin GS, are the most abundant group of peptides isolated from *Conus* venoms so far. This structural class encompasses at least five known pharmacological classes — ω conotoxin calcium-channel blockers, δ conotoxins which inhibit the inactivation of sodium channels, κ conotoxin PVIIA which blocks potassium channels, the sodium-channel blocker conotoxin GS and two peptides recently found in *Conus marmoreus* that affect both sodium and calcium currents [20,30,41]. Only the solution structures of ω conotoxins have previously been determined, and these have revealed a triple-stranded antiparallel β sheet with +2*x*, –1 topology and cystine-knot motif common to a number of toxic and inhibitory peptides [34,42].

In this study, we have compared the solution structures of conotoxin GS, ω conotoxin GVIA [43–46] and μ agatoxin I [47] to highlight structural differences and identify features that may be important for their different target specificities. The N-type calcium-channel antagonist from *C. geographus*, ω conotoxin GVIA, has been the most studied of all conotoxins and extensive structural and activity data have been reported. The toxin from the venom of the American funnel web spider *Agelenopsis aperta*, μ agatoxin I, modifies the kinetics of insect neuronal sodium channels. The solution structure of conotoxin GS has a similar global fold to both ω conotoxin GVIA and μ agatoxin I (Fig. 8). In spite of their different amino acid sequences, the Cα atoms of the six conserved half-cystines superimpose with an rms deviation of 0.91 Å between conotoxin GS and ω GVIA and 0.81 Å between conotoxin GS and μ agatoxin I. All these molecules contain a type II β turn in loop 1, and conotoxin GS and μ agatoxin I also have a type II turn in loop 3. However, several local differences

Figure 8

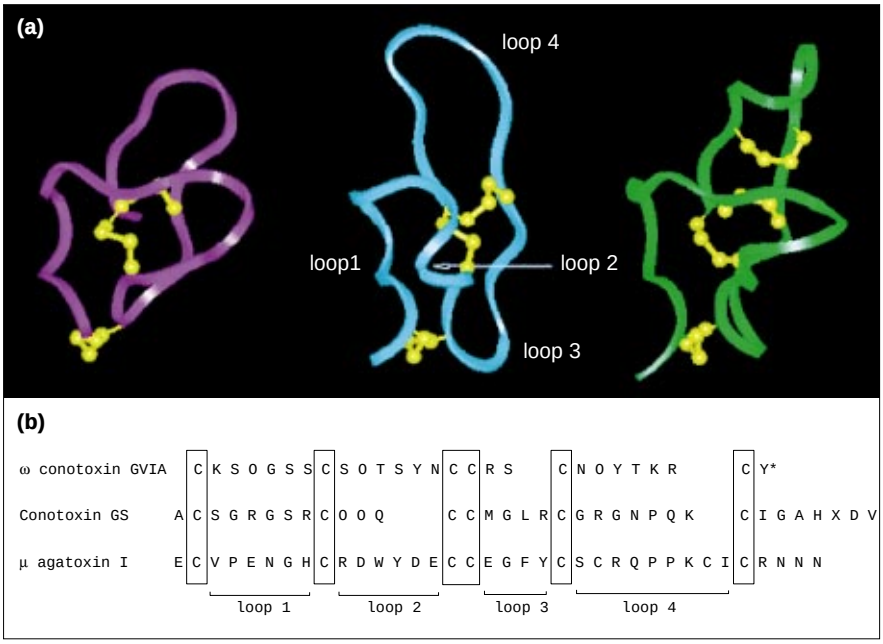

The solution structures of ω conotoxin GVIA, conotoxin GS and μ agatoxin I.
(a) Comparison of the Cα ribbon diagrams of ω conotoxin GVIA (purple), conotoxin GS (blue) and μ agatoxin I (green). The structural alignment shown is based on a superimposition of the Cα atoms of the six conserved half-cystines involved in the cystine-knot motif. The disulfide bonds are shown in yellow. For clarity, the C-terminal seven residues of conotoxin GS and four residues of μ agatoxin I are not shown. The coordinates for GVIA [43] (accession code 1OMC) and μ agatoxin I [47] (accession code 1EIT) were obtained from the PDB.
(b) Polypeptide sequences aligned on the basis of the six conserved half-cystine positions; O is γ-*trans*-L-hydroxyproline; X is γ-carboxy-L-glutamic acid; * is an amidated C terminus. Note that μ agatoxin I contains a fourth disulfide bond in loop 4.

in backbone conformation were observed. In conotoxin GS, the first strand consists solely of a β bridge at Ser7, and does not constitute a complete β sheet. Several previous studies have emphasized deviations from classical β-sheet structure in small disulfide-rich polypeptides [39,44,46], but this appears to be further exacerbated in conotoxin GS by a tight turn following the first β strand.

Several other structural differences between these molecules result from changes in the size of loops 2 and 4, which are manifest in the relative orientation of these loops in the three-dimensional structures (Fig. 8). In particular, loop 2 of conotoxin GS lacks three residues relative to both ω conotoxin GVIA and μ agatoxin I and has a markedly different conformation. In conotoxin GS, these residues form a tight turn in place of a series of overlapping turns in both ω conotoxin GVIA and μ agatoxin I. The tight turn in conotoxin GS is necessary to bring Cys13 into the correct orientation to form a disulfide bridge with Cys27. The significant structural difference in loop 2 between ω conotoxin GVIA and conotoxin GS, which are calcium and sodium channel blockers, respectively, is of interest because this region incorporates residues suggested to be involved in binding and calcium-channel subtype discrimination by the ω conotoxins [48]. Furthermore, a striking difference is observed in the relative orientation of loops 2 and 4 in the structures. In conotoxin GS, loop 4 protrudes from the core of the molecule and is relatively disordered, lacking long-range interactions that were observed for this region of ω GVIA and μ agatoxin I.

Biological implications

Voltage-dependent sodium channels are intrinsic membrane proteins that play an important role in fast communication in excitable cells. A short stretch of amino acids, the pore region, is the sole determinant of sodium selectivity and also forms the binding site for many channel blockers. Toxins that interact intimately with this region can be used as structural templates to deduce the spatial organization of the pore region of sodium channels. These models of pore structure are valuable for understanding the mechanisms of ion permeation, and may ultimately be useful for the rational design of drugs that could modify the function of ion channels in patients with ischaemic injury to the heart or brain.

The piscivorous cone snail *Conus geographus* produces two different polypeptide toxins, the **μ** conotoxins and conotoxin GS, which inhibit voltage-dependent sodium channel function. Conotoxin GS has a six-cysteine and four-loop structure, whereas the **μ** conotoxins contain a six-cysteine and three-loop structural framework. Both toxins bind to skeletal muscle sodium channels to prevent sodium ion conduction. In this study, we have determined the three-dimensional solution structure of the 34-residue polypeptide conotoxin GS. The structure consists of a **β** hairpin and several turns, which are cross-linked by three disulfide bonds. The turns contain several cationic and polar residues that may be important for interacting with the sodium channel. An interesting feature of conotoxin GS is the presence of the two post-translationally modified amino acids, **γ**-*trans*-hydroxyproline and

γ-carboxyglutamic acid. The *cis*-peptide bond conformation of all the hydroxyproline and proline residues in conotoxin GS, suggests a structural significance for this geometry in the protein. Although γ-carboxyglutamic acid residues have been implicated previously in the binding of calcium ions and membranes, the role of this residue in conotoxin GS is not obvious. As the sequence and structure of conotoxin GS are considerably different to those of the μ conotoxins, it provides a valuable new probe for further characterization of sodium-channel geometry. The structure of conotoxin GS will facilitate the design of analogs to define the channel binding surface and provides direction for complementary mutagenesis on the sodium channel to identify the interacting residues. These experiments with conotoxins may prove as useful in modelling the outer vestibule of sodium channels as the peptide toxins from scorpions have been in studies of potassium channels.

Materials and methods

Peptide synthesis

Boc-L-amino acids were obtained from Novabiochem (Läufelfingen, Switzerland) or Peptide Institute (Osaka, Japan). *t*-Boc-Val-OCH_2-PAM-resin was obtained from Applied Biosystems (Foster City, CA). 2-(1H-benzotriazol-1-yl)-1,1,3,3-tetramethyluronium hexafluorophosphate (HBTU) was obtained from Richelieu Biotechnologies (Quebec, Canada). Other reagents were of peptide synthesis grade obtained from Auspep (Melbourne, Australia).

Conotoxin GS and [Glu32]conotoxin GS were assembled manually by stepwise solid-phase-peptide synthesis using an *in situ* neutralisation protocol for Boc chemistry [49]. The following sidechain protection was used: Arg(Tos), Asp(OcHxl), Cys(MeBzl), $Gla(OcHxl)_2$, Glu(OcHxl), His(DNP), Hyp(Bzl), Lys(2-ClZ) and Ser(Bzl). The dinitrophenyl protecting group was removed from histidine using a solution of 20% 2-mercaptoethanol, 10% N,N-diisopropylethylamine (DIEA) in N,N-dimethylformamide (DMF) (2×30 min). The peptides were then cleaved from the resin and simultaneously deprotected by treatment with anhydrous HF/*p*-cresol/*p*-thiocresol (18:1:1 v/v, 0°C, 90 min). The crude peptide products were precipitated with diethyl ether, dissolved in 50% aqueous acetic acid, diluted with water and lyophilized. Purification was achieved by preparative reverse-phase HPLC (Vydac C18 column, 22×250 mm) using a linear gradient of 0–60% acetonitrile in water and 0.1% trifluoroacetic acid over 60 min. The purified reduced peptides were oxidised at room temperature for 24 h in 0.1 M ammonium acetate buffer (pH 7.8), at a peptide concentration of 3.6×10^{-5} M in the presence of reduced (GSH) and oxidised (GSSG) glutathione [15]. The molar ratio of peptide:GSH:GSSG was1:50:5. The oxidised products were purified by preparative reverse-phase HPLC using the same gradient and solvent system as previously described. This procedure yielded 16% and 11% of purified oxidised conotoxin GS and [Glu32]conotoxin GS, respectively, based on the starting resin. Analytical reverse-phase HPLC (Vydac C_{18} column, 4.6×150 mm) and electrospray ionisation mass spectrometry (Perkin Elmer-Sciex API III instrument) confirmed the purity and molecular weights of the synthetic peptides.

NMR spectroscopy

Samples for ^{1}H-NMR measurements contained 2 mM peptide in one of the following 99.99% D_2O or 90% H_2O/10% D_2O (v/v) at pH 2.9, 30% d_3-TFE/70% H_2O or 90% H_2O/10% D_2O (pH 5.4) with ratios of $CaCl_2$ to peptide of 1:1, 5:1 and 10:1. Spectra were recorded at 25°C and 15°C on a Bruker ARX-500 spectrometer equipped with a z-gradient unit. 2D-NMR spectra were recorded in phase-sensitive mode using time-proportional phase incrementation for quadrature detection in the t_1 dimension [50]. The 2D experiments, as reviewed in [24,27], included DQF-COSY, E-COSY, TOCSY using a MLEV-17 spin lock sequence with a mixing time of 80 ms and NOESY with mixing times of 100 ms, 250 ms and 350 ms. For DQF-COSY and E-COSY experiments, solvent suppression was achieved using selective low-power irradiation of the water resonance during a relaxation delay of 1.8 s. Solvent suppression for TOCSY and NOESY experiments was achieved using a modified WATERGATE sequence, as previously described in [19]. Slowly exchanging NH protons were detected by acquiring a series of 1D and TOCSY spectra of the fully protonated peptide immediately following dissolution in D_2O.

Spectra were acquired over 6024 Hz with 4096 complex data points in F_2 and 400–600 increments in F_1, with 16 to 64 scans per increment. All spectra were processed using UXNMR (Bruker). The t_1 dimension was zero-filled to 2048 real data points, and 90° phase-shifted sine bell window functions were applied in both dimensions followed by Fourier transformation and fifth order polynomial baseline correction. Chemical shifts were referenced to external 2,2-dimethyl-2-silapentane-5-sulfonate (DSS). $^3J_{H\alpha-H\beta}$ coupling constants were measured from E-COSY spectra and $^3J_{NH-H\alpha}$ coupling constants were measured from high resolution 1D spectra and DQF-COSY spectra, which was strip-transformed to 8K×1K. 1D slices from the DQF-COSY spectrum were analysed using a simple peak-simulation routine to obtain approximate coupling constants.

^{1}H-^{13}C HMQC [51] and HMQC-TOCSY [52] spectra were recorded for a 4 mM peptide sample in 99.99% D_2O. Spectral widths in the ^{1}H and ^{13}C dimensions were 5050 Hz and 18 864 Hz, respectively, and 4096 complex data points were acquired with 256 F_1 increments. The ^{13}C HMQC and ^{13}C HMQC-TOCSY spectra were accumulated with 48 and 128 scans per increment.

Structural restraints

Distance restraints were derived from the 250 ms NOESY spectrum recorded at 25°C. Cross peak volumes were classified as strong, medium, weak or very weak, corresponding to upper bound interproton distance restraints of 2.7, 3.5, 5.0 and 6.0 Å, respectively. Appropriate pseudoatom corrections were applied to nonstereospecifically assigned methylene and methyl protons [24]. Backbone dihedral angle restraints were inferred from $^3J_{NH-H\alpha}$ coupling constants, with ϕ restrained to $-120\pm40°$ for a $^3J_{NH-H\alpha}$ greater than 8 Hz and to $-65\pm25°$ for a $^3J_{NH-H\alpha}$ less than 5 Hz. χ_1 angles for several amino acid residues were restrained on the basis of the relative magnitude of NH–Hβ and Hα–Hβ NOEs and $^3J_{H\alpha-H\beta}$ coupling constants [27]. Peptide bond ω angles were set to *trans* with the exception of Cys9–Hyp10, Hyp10–Hyp11 and Asn23–Pro24, which were set to the *cis* configuration. Hydrogen bonds were identified from a combined analysis of the amide proton exchange rates and the initial structures. Nine hydrogen bonds were identified unambiguously and restrained — 3NH–12CO, 7NH–4CO, 14NH–3CO, 17NH–14CO, 18NH–28CO, 20NH–26CO, 26NH–20CO, 27NH–7CO and 28NH–18CO. For each hydrogen bond, the NH–O and N–O distances were set to 2.3 and 3.2 Å, respectively.

Structure calculations

Three-dimensional structures were calculated using a simulated annealing and energy minimisation protocol in the program X-PLOR version 3.1 [53]. Starting structures with randomised ϕ and ψ angles and extended side chains were generated using an *ab initio* simulated annealing protocol [54]. The disulfide bonds were included as pseudo-NOE restraints and the simulated annealing protocol consisted of 20 ps of high temperature molecular dynamics (1000K), with a low weighting on the repel force constant and NOE restraints. This was followed for a further 10 ps with an increased force constant on the experimental NOE restraints. The disulfide bonds were then formally included and the dihedral force constant increased prior to cooling the system to 300K and increasing the repel force constant over 15 ps of dynamics.

Refinement of these structures was achieved using the conjugate gradient Powell algorithm with 1000 cycles of energy minimization and a refined forcefield based on the program CHARMm [55]. Structures were analysed using PROCHECK [56], PROMOTIF [31] and SSTRUC (D Smith, personal communication), and displayed using Insight II (version 95.0.3, Biosym Technologies, San Diego, CA), GRASP [57] and MOLSCRIPT [58].

Accession numbers

The NMR restraints and coordinates of the 20 final structures have been deposited at the Brookhaven Protein Data Bank (code 1ag7).

Supplementary material

Supplementary material contains a Table of ^{1}H and ^{13}C resonance assignments and a Figure showing ^{1}H-^{13}C HMQC spectrum of conotoxin GS.

Acknowledgements

This work was supported in part by a grant from the Australian Research Council (DJC) and an Australian Postgraduate Award (JMH). We thank Martin Scanlon for helpful discussions.

References

1. Strichartz, G., Rando, T. & Wang, G.K. (1987). An integrated view of the molecular toxinology of sodium channel gating in excitable cells. *Annu. Rev. Neurosci.* 10, 237–267.
2. Catterall, W.A. (1988). Structure and function of voltage-sensitive ion channels. *Science* 242, 50–61.
3. Noda, M., Suzuki, H., Numa, S. & Stühmer, W. (1989). A single point mutation confers tetrodotoxin and saxitoxin insensitivity on the sodium channel II. *FEBS Lett.* 259, 213–216.
4. Terlau, H., *et al.*, & Numa, S. (1991). Mapping the site of block by tetrodotoxin and saxitoxin of sodium channel II. *FEBS Lett.* 293, 93–96.
5. Stephan, M.M., Potts, J.F. & Agnew, W.S. (1994). The μI skeletal muscle sodium channel: mutation E403Q eliminates sensitivity to tetrodotoxin but not to μ-conotoxins GIIIA and GIIIB. *J. Membr. Biol.* 137, 1–8.
6. Lipkind, G.M. & Fozzard, H.A. (1994). A structural model of the tetrodotoxin and saxitoxin binding site of the Na^+ channel. *Biophys. J.* 66, 1–13.
7. Dudley, S.C., Todt, H., Lipkind, G. & Fozzard, H.A. (1995). A μ-conotoxin-insensitive Na^+ channel mutant: possible localisation of a binding site at the outer vestibule. *Biophys. J.* 69, 1657–1665.
8. Chahine, M., *et al.*, & Kallen, R.G. (1995). Characterising the μ-conotoxin binding site on voltage-sensitive sodium channels with toxin analogs and channel mutations. *Recept. Channels* 3, 161–174.
9. Sato, S., Nakamura, H., Ohizumi, Y., Kobayashi, J. & Hirata, Y. (1983). The amino acid sequences of homologous hydroxyproline-containing myotoxins from the marine snail *Conus geographus* venom. *FEBS Lett.* 155, 277–280.
10. Cruz, L.J., *et al.*, & Moczydlowski, E. (1985). *Conus geographus* toxins that discriminate between neuronal and muscle sodium channels. *J. Biol. Chem.* 260, 9280–9288.
11. Yanagawa, Y., Abe, T., Satake, M., Odani, S., Suzuki, J. & Ishikawa, K. (1988). A novel sodium channel inhibitor from *Conus geographus*: purification, structure, and pharmacological properties. *Biochemistry* 27, 6256–6262.
12. Moczydlowski, E., Olivera, B.M., Gray, W.R. & Strichartz, G.R. (1986). Discrimination of muscle and neuronal Na-channel subtypes by binding competition between [^{3}H]saxitoxin and μ conotoxins. *Proc. Natl. Acad. Sci. USA* 83, 5321–5325.
13. Ohizumi, Y., Nakamura, H., Kobayashi, J. & Catterall, W.A. (1986). Specific inhibition of [^{3}H]saxitoxin binding to skeletal muscle sodium channels by geographutoxin II, a polypeptide channel blocker. *J. Biol. Chem.* 261, 6149–6152.
14. Chen, L.-Q., Chahine, M., Kallen, R.G., Barchi, R.L. & Horn, R. (1992). Chimeric study of sodium channels from rat skeletal and cardiac muscle. *FEBS Lett.* 309, 253–257.
15. Nakao, M., Nishiuchi, Y., Nakata, M., Watanabe, T.X., Kimura, T. & Sakakibara, S. (1995). Synthesis and disulfide structure determination of conotoxin GS, a γ-carboxyglutamic acid-containing neurotoxic peptide. *Letters in Peptide Science* 2, 17–26.
16. Lancelin, J.-M., *et al.*, & Inagaki, F. (1991). Tertiary structure of conotoxin GIIIA in aqueous solution. *Biochemistry* 30, 6908–6916.
17. Ott, K.-H., Becker, S., Gordon, R.D. & Rüterjans, H. (1991). Solution structure of μ-conotoxin GIIIA analysed by 2D-NMR and distance geometry calculations. *FEBS Lett.* 278, 160–166.
18. Wakamatsu, K., *et al.*, & Sato, K. (1992). Structure–activity relationships of μ-conotoxin GIIIA: structure determination of active and inactive sodium channel blocker peptides by NMR and simulated annealing calculations. *Biochemistry* 31, 12577–12584.
19. Hill, J.M., Alewood, P.F. & Craik, D.J. (1996). Three-dimensional solution structure of μ-conotoxin GIIIB, a specific blocker of skeletal muscle sodium channels. *Biochemistry* 35, 8824–8835.
20. Myers, R.A., Cruz, L.J., Rivier, J.E. & Olivera, B.M. (1993). *Conus* peptides as chemical probes for receptors and ion channels. *Chem. Rev.* 93, 1923–1936.
21. Prorok, M., Warder, S.E., Blandl, T. & Castellino, F.J. (1996). Calcium binding properties of synthetic γ-carboxyglutamic acid-containing marine cone snail 'sleeper' peptides, conantokin-G and conantokin-T. *Biochemistry* 35, 16528–16534.
22. Skjaerbaek, N., Nielsen, K.J., Lewis, R.J., Alewood, P. & Craik, D.J. (1997). Determination of the solution structures of conantokin-G and conantokin-T by CD and NMR spectroscopy. *J. Biol. Chem.* 272, 2291–2299.
23. Nakamura, T., Yu, Z., Fainzilber, M. & Burlingame, A.L. (1996). Mass spectrometric-based revision of the structure of a cysteine-rich peptide toxin with γ-carboxyglutamic acid, from the sea snail, *Conus textile*. *Protein Sci.* 5, 524–530.
24. Wüthrich, K. (1986). *NMR of Proteins and Nucleic Acids*, Wiley-Interscience, New York.
25. Wüthrich, K., Tun-kyi, A. & Schwyzer, R. (1972). Manifestation in the ^{13}C-NMR spectra of two different molecular conformations of a cyclic pentapeptide. *FEBS Lett.* 25, 104–108.
26. Garbay-Jaureguiberry, C., Arnoux, B., Prangé, T., Wehri-Altenburger, S., Pascard, C. & Roques, B.P. (1980). X-ray and NMR studies of L-4-hydroxyproline conformation in oligopeptides related to collagen. *J. Am. Chem. Soc.* 102, 1827–1837.
27. Wagner, G. (1990) NMR investigations of protein structure. *Prog. NMR Spectrosc.* 22, 101–139.
28. Wishart, D.S., Sykes, B.D. & Richards, F.M. (1992). The chemical shift index: a fast and simple method for the assignment of protein secondary structure through NMR spectroscopy. *Biochemistry* 31, 1647–1651.
29. Klaus, W., Broger, C., Gerber, P. & Senn, H. (1993). Determination of the disulfide bonding pattern in proteins by local and global analysis of nuclear magnetic resonance data. *J. Mol. Biol.* 232, 897–906.
30. Cruz, L.J. (1996). Primary structural motifs of *Conus* peptides. In *Natural Toxins II*. (Singh, B.R. & Tu, A.T., eds), pp. 155–167, Plenum Press, New York.
31. Hutchinson, E.G. & Thornton, J.M. (1996). PROMOTIF: a program to identify and analyse structural motifs in proteins. *Protein Sci.* 5, 212–220.
32. Lewis, P.N., Momany, F.A. & Scheraga, H.A. (1973). Chain reversals in proteins. *Biochem. Biophys. Acta* 303, 211–229.
33. Wilmot, C.M. & Thornton, J.M. (1990). β-Turns and their distortions: a proposed new nomenclature. *Protein Eng.* 3, 479–493.
34. Pallaghy, P.K., Nielsen, K.J., Craik, D.J. & Norton, R.S. (1994). A common structural motif incorporating a cystine knot and a triple-stranded β sheet in toxic and inhibitory polypeptides. *Protein Sci.* 3, 1833–1839.
35. Stewart, D.E., Sarkar, A. & Wampler, J.E. (1990). Occurrence and role of *cis* peptide bonds in protein structures. *J. Mol. Biol.* 214, 253–260.
36. MacArthur, M.W. & Thornton, J.M. (1991). Influence of proline residues on protein conformation. *J. Mol. Biol.* 218, 397–412.
37. Sato, K., *et al.*, & Inagaki, F. (1991). Active site of μ-conotoxin GIIIA, a peptide blocker of muscle sodium channels. *J. Biol. Chem.* 266, 16989–16991.
38. Becker, S., Prusak-Sochaczewski, E., Zamponi, G., Beck-Sickinger, A.G., Gordon, R.G. & French, R.J. (1992). Action of derivatives of μ-conotoxin GIIIA on sodium channels. Single amino acid substitutions in the toxin separately affect association and dissociation rates. *Biochemistry* 31, 8229–8238.
39. Reily, M.D., Thanabal, V. & Adams, M.E. (1995). The solution structure of ω-Agatoxin-IVB, a P-type calcium channel antagonist from venom of the funnel web spider, *Agelenopsis aperta*. *J. Biomol. NMR* 5, 122–132.
40. Kim, J.I., *et al.*, & Arata, Y. (1995). Three-dimensional solution structure of the calcium channel antagonist ω-agatoxin IVA: consensus molecular folding of calcium channel blockers. *J. Mol. Biol.* 250, 659–671.

41. Terlau, H., Shon, K.-J., Grilley, M., Stocker, M., Stühmer, W. & Olivera, B.M. (1996). Strategy for rapid immobilisation of prey by a fish-hunting marine snail. *Nature* **381**, 148–151.
42. Narasimhan, L., Singh, J., Humblet, C., Guruprasad, K. & Blundell, T. (1994). Snail and spider toxins share a similar tertiary structure and 'cysteine motif'. *Nat. Struct. Biol.* **1**, 850–852.
43. Davis, J.H., Bradley, E.K., Miljanich, G.P., Nadasdi, L., Ramachandran, J. & Basus, V.J. (1993). Solution structure of ω-conotoxin GVIA using 2D NMR spectroscopy and relaxation matrix analysis. *Biochemistry* **32**, 7396–7405.
44. Pallaghy, P.K., Duggan B.M., Pennington, M.W. & Norton, R.S. (1993). Three-dimensional structure in solution of the calcium channel blocker ω-conotoxin. *J. Mol. Biol.* **234**, 405–420.
45. Sevilla, P., Bruix, M., Santoro, J., Gago, F., Garcia, A.G. & Rico, M. (1993). Three-dimensional structure of ω-conotoxin GVIA determined by ^{1}H NMR. *Biochem. Biophys. Res. Commun.* **192**, 1238–1244.
46. Skalicky, J.J., Metzler, W.J., Ciesla, D.J., Galdes, A. & Pardi, A. (1993), Solution structure of the calcium channel antagonist ω-conotoxin GVIA. *Protein Sci.* **2**, 1591–1603.
47. Omecinsky, D.O., Holub, K.E., Adams, M.E. & Reily, M.D. (1996). Three-dimensional structure analysis of μ-agatoxins: further evidence for common motifs among neurotoxins with diverse ion channel specificities. *Biochemistry* **35**, 2836–2844.
48. Nadasdi, L., Yamashiro, D., Chung, D., Tarczy-Hornoch, K., Adriaenssens, P. & Ramachandran, J. (1995). Structure–activity analysis of a *Conus* peptide blocker of N-type neuronal calcium channels. *Biochemistry* **34**, 8076–8081.
49. Schnölzer, M., Alewood, P., Jones, A., Alewood, D. & Kent, S.B.H. (1992). *In situ* neutralisation in Boc-chemistry solid phase peptide synthesis. *Int. J. Pept. Protein Res.* **40**, 180–193.
50. Marion, D. & Wüthrich, K. (1983). Measurement of phase sensitive two-dimensional correlated spectroscopy (COSY) for measurements of ^{1}H-^{1}H spin-spin coupling constants in proteins. *Biochem. Biophys. Res. Commun.* **113**, 967–974.
51. Bax, A., Griffey, R.H. & Hawkins, B.L. (1983). Correlation of proton and nitrogen-15 chemical shifts by multiple quantum NMR. *J. Magn. Reson.* **55**, 301–315.
52. Lerner, L. & Bax, A. (1986). Sensitivity-enhanced two-dimensional heteronuclear relayed coherence transfer NMR spectroscopy. *J. Magn. Reson.* **69**, 375–380.
53. Brünger, A.T. (1992). X-PLOR Manual Version 3.1, Yale University, New Haven, CT, USA.
54. Nilges, M., Gronenborn, A.M., Brünger, A.T. & Clore, G.M. (1988). Determination of three-dimensional structures of proteins by simulated annealing with interproton distance restraints. Application to crambin, potato carboxypeptidase inhibitor and barley serine proteinase inhibitor 2. *Protein Eng.* **2**, 27–38.
55. Brooks, B.R., Bruccoleri, R.E., Olafson, B.D., States, D.J., Swaminathan, S. & Karplus, M. (1983). CHARMM: a program for macromolecular energy, minimisation and dynamics calculations. *J. Comput. Chem.* **4**, 187–217.
56. Laskowski, R.A., MacArthur, M.W., Moss, D.S. & Thornton, J.M. (1993). PROCHECK: a program to check the stereochemical quality of protein structure coordinates. *J. Appl. Cryst.* **26**, 283–291.
57. Nicholls, A., Sharp, K.A. & Honig, B. (1991). Protein folding and association: insights from the interfacial and thermodynamic properties of hydrocarbons. *Proteins* **11**, 281–296.
58. Kraulis, P. (1991). MOLSCRIPT: a program to produce both detailed and schematic plots of protein structures. *J. Appl. Cryst.* **24**, 946–950.